Studies and cross-comparisons of severe accident prevention and mitigation capabilities of a SFR and a GFR

Frédéric Bertrand, A. Bachrata, N. Seiler, Jean-Baptiste Droin, A Mouly

STUDIES AND CROSS-COMPARISONS OF SEVERE ACCIDENT PREVENTION AND MITIGATION CAPABILITIES OF A SFR AND A GFR

Bertrand F, Bachrata A, Seiler N, Droin J.B, Mouly A
CEA, DES, IRESNE, DER
F-13108 Saint Paul Lez Durance, France
frederic.bertrand@cea.fr

ABSTRACT

CEA has developed Generation IV fast neutron reactors with gas and sodium coolants in the two last tenth of years. Namely these reactor projects were the GFR2400 (gas-cooled fast reactor of 2400 thermal megawatts) and ASTRID (sodium-cooled fast reactor demonstrator of 1500 thermal megawatts). The objective of this paper is to provide a cross-comparison of the severe accident prevention and mitigation capability of these reactor concepts based on the work done during a significant time period and taking benefit of the distance since these studies. This comparison can highlight both generic trends resulting from a common study approach used for both concepts and from very detailed results obtained during their conceptual design studies. Despite their power difference and their fuel element design specificities, the main study results and conclusions are quite generical of the two concepts as explained in the paper. Thus they could be extrapolated to other reactor design providing main reactor features are kept (core materials, coolant, neutron spectrum, etc.). The assessment of core melting prevention relies on the study of the natural behavior of the GFR2400 and of ASTRID when facing the various accident sequence families. Then, the efficiency and the features of the systems to be foreseen for core degradation prevention are presented. As far as mitigation is concerned, all the consequences of core melting are investigated (i.e. the induced loadings in terms of nature and of range) by considering various core degraded states. Based on the magnitude of these loadings, the needs of mitigation means are assessed for each concept. Among other trends, the presented work shows the very good prevention capability of the SFR concept but the necessity to mitigate the fast vaporization and expansion of degraded core materials. Conversely, the limited coolant capability of the GFR concept and its low thermal inertia require a pressurized gas circulation into the core, limiting its prevention capability whereas its core melting should not induce substantial mechanical loadings of the reactor structures. However, for this last concept, thermochemical interactions between the core materials are an issue deeply investigated in order to understand and simulate core degradation.

KEYWORDS

Severe accidents, Prevention, Mitigation, SFR, GFR, Gen IV

GLOSSARY

(B)DBA	Beyond design basis accident
CC	Close containment
CFV	Low void worth core
CRA	Control rod assembly
CRW	Control rod withdrawal
DCS-M-TT	Safety mitigation complementary device-transfer tube
DHR	Decay heat removal
FP	Fission product
HT	Hexagonal tubes (hexcan)
IHX	Intermediate heat exchanger
LB-LOCA	Loss of coolant accident (large break)
LOF	Loss of flow
LOFA	Loss of flow accident
LOHS	Loss of heat sink
LOOP	Loss of off-site power
PCS	Power conversion system
PCT	Peak clad temperature
RHP	Reactor high pressure DHR system
RLP	Reactor low pressure DHR system
SA	Sub-assembly
SAF	Sub-assembly fault
SB-LOCA	Loss of coolant accident (small break)
SG	Steam generator
TLOP	Total loss of power
TOP	Transient overpower
U(xxx)	Unprotected xxx (transient without reactor shutdown)

NOMENCLATURE

$\dot{m}$	Core flow rate ($kg.s^{-1}$)
C_p	Heat capacity ($J.kg^{-1}.K^{-1}$)
E_{meca}	Expansion mechanical energy or work (J)
P	Core power (w)
P_f	Final gas or vapor expansion pressure (Pa)
P_i	Initial gas or vapor expansion pressure (Pa)
Q	Power removed by the coolant (w)
T_{in}	Core inlet temperature (K)
T_{out}	Core outlet temperature (K)
V_f	Final gas or vapor expansion volume (m^3)
V_i	Initial gas or vapor expansion volume (m^3)
γ	Heat capacity ratio (-)

1. INTRODUCTION

Since Generation IV forum deals with R&D sharing for the development of various reactor concepts whose goal, among others, is to improve and to make friendly understandable safety, it is expected to have some cross-comparison between concepts, in particular dealing with accident behavior and safety. Some criteria enabling a comparison of different Gen IV reactor concepts are proposed by Bertrand et al. (2020). This comparison relies on the expected accidental behavior of the reactor considered based on coolant features, core/fuel features and the consequent loadings on physical barriers confining fission products. As a result, it is very simple and enables, when designing a reactor, to have a first idea of its accidental behavior without making extensive safety studies since this analysis relies on order of magnitudes. When first design choices have been done, in the aim to go further in the analysis of accidental behavior, more detailed comparisons are needed. The current paper deals once again with cross-comparison of reactor concepts but it is carried-out at a more advanced stage of the design and is only limited to comparison of the gas-cooled fast reactor concept (GFR 2400 developed at CEA in the years 2000's (Malo et al., 2008)) with the sodium-cooled fast reactor concept (ASTRID (Le Coz et al., 2013) developed in the years 2010's). Actually, in the comparison presented in the current paper relying on detailed study and calculation results, only Gen IV concepts onto which CEA has put substantial efforts are considered. Despite the power difference of the considered reactor concept the feed-back of the studies performed at CEA for a GFR demonstrator (ALLEGRO) and for SFR SFR of larger or smaller power level, the major trends obtained in this article are quite generical and could be extrapolated to other reactor design providing main basic options remain the same (core materials and volumic power, coolant features, system architecture (pool/loop), etc. One of the main interest of this comparison lies in the realization of the studies in the same frame and with the same approach, consisting first in an investigation of prevention of core melting capability as well as in mitigation of core melting consequences capability. The distance taken since this time enables to present the results in a synthetic way, based more or less on the same level of study deepness, and therefore, only the important findings are highlighted. In section 2 of the paper, an overview of the two considered reactor concepts is presented. Then, section 3 is dedicated to the behavior of the reactors in case of very challenging situations in order to identify the sequences leading to core melting. Section 4 is dedicated to severe accident consequences for both reactor concepts by presenting investigations related to various core degraded states and then related to core melting initiating sequences. The degraded state situations analysis enables to quantify the order of magnitudes of the various effects associated to core degradation. Additionally, the event sequence analysis, starting from the event initiating the accident, enables to check the adequacy of the design of mitigation devices. Finally a synthesis of this cross-comparison is drawn in section 5.

Finally, this paper provides first a generic frame to compare some reactor concepts (when design is under progress) or reactor design in terms of prevention and mitigation of severe accidents. It enables to quantify and to support some qualitative assessments related to basis design options of reactor concepts (nature of coolant, core materials, prevention and mitigation devices). The conclusion and insights of the article bring out some general trends relative to gas-cooled and to liquid metal cooled fast spectrum reactors. The comparison methodology presented here, that is based on studies of elementary physical consequences of accidents and then to transient studies could be applied to other Gen IV innovative concept during their design, in order to support it.

2. OVERVIEW OF CONSIDERED REACTOR DESIGNS

The reactor concepts considered in order to quantify the criteria proposed in this paper are roughly described in this section. The presentation here focuses on the main features required to understand the calculation background, that is to say the core and the main systems for core cooling. For further elements, some references are provided in the section.

2.1 GFR 2400 reactor design (Gas-cooled fast reactor, 2400 thermal megawatts)

The GFR represents a promising and attractive fourth generation (GEN IV) concept, combining the benefits of a fast spectrum and of a high temperature (~850 ◦C at the core outlet). The GFR concept is clearly innovative compared to other reactor concepts and no demonstrator has been ever built. The project of an industrial GFR has to address key R&D challenges, especially regarding, the fuel technology and core performance and the safety (in particular the decay heat removal (DHR) issue). The operating point of the 3-loops reactor at full nominal power enables to convert the 2400 MWth delivered by the core in 1100 MWe, partly by secondary circuit turbomachines (auxiliary alternators: 3 x 130 MWe) and partly by a steam turbine (main alternator: 1 x 730 MWe) settled in the ternary circuit (Fig 1). The resulting cycle efficiency is very close to 45 %. The secondary circuit is filled with a mixture of helium (to favour the heat exchanges) and nitrogen (to favour the efficiency and the design of the turbomachines); the ternary circuit is filled with water, vaporized in 3 steam generators according to a classical Rankine cycle. The primary system arrangement (Fig 2) includes the reactor vessel, the 3 main primary loops (PCS loops) and their heat exchangers (IHX) as well as the DHR loops permitting to cool the core in accidental situations. Actually, there are three loops for the Reactor High Pressure cooling system (RHP) and a loop for the low pressure system (RLP). The secondary side of the DHR loops, each one being able to remove 100 % of the decay heat after the reactor scram, is filled with water pressurized at 10 bars. These secondary DHR loops are cooled via an exchanger immersed in a pool. Each pool associated to a loop can remove the residual power during 24 hours without being refilled. Moreover, all the previous components are enclosed in a close containment (CC) which keeps the primary inventory in case of loss of coolant accident (LOCA). The CC is filled with nitrogen at 1 bars, except in LOCA situation. This CC is in its turn enclosed in the Containment Building (CB) whose free volume is assumed to be equal to 60 000 m^3 in our reference configuration. Two fuel concepts have been investigated: a plate type and a more classical pin type. The present paper only deals with the plate type associated to more study results (Fig 3). The plate-type fuel element is an innovative concept based on two ceramic plates which encloses a honeycomb structure containing the fuel cylindrical pellets (in red on Figure 3). The plate consists in uranium–plutonium–minor actinide carbide, (U,Pu,MAs)C for fuel pellets, composite SiC-SiCf for thin plates (clad in grey on Figure 3) and SiC for the honeycomb structure. It appeared necessary to add a leak-tight barrier to prevent the Fission Products (FP) diffusion through the clad. The fuel plates are cooled with helium along the plate that are integrated in baskets of about 40 cm high implemented in hexcans encompassing the whole SA (Fig. 3). The current reference choice for this inner liner is a 50 µm layer of W-14Re. At the hot spot of the core, the clad temperature is equal to 1000°C and the fuel temperature is about 1380°C in nominal conditions. The plates are arranged in baskets superposed in hexagonal tubes (HT) permitting to differentiate the flow rate depending on the power factor distribution within the core.

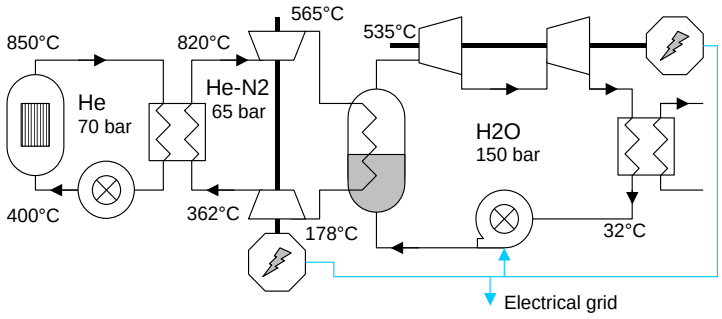

Fig. 1 Nominal operating point of the GFR (Malo et al., 2008)

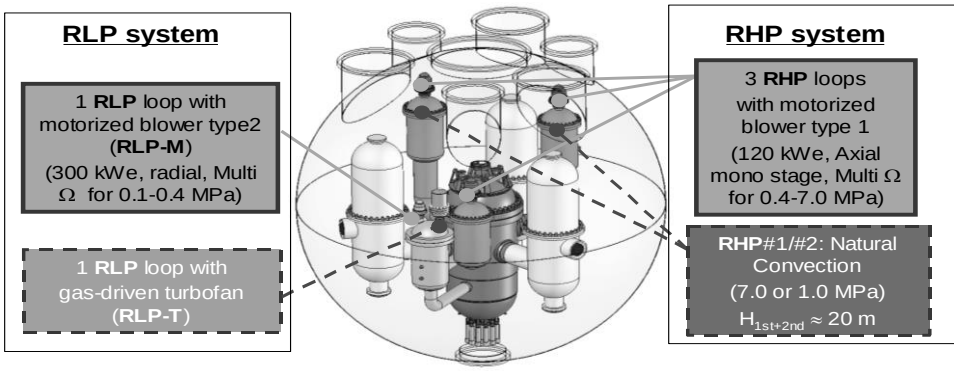

Fig. 2 Arrangement of the primary circuit components (Malo et al., 2008)

The height of the core is of 2.35 m and its diameter is of 3.8 m, thus corresponding to a power density of about 90 MW/m^3. The head loss across the core has been minimized at a value of 1.4 bars at the nominal regime in order to favour natural circulation in DHR regime.

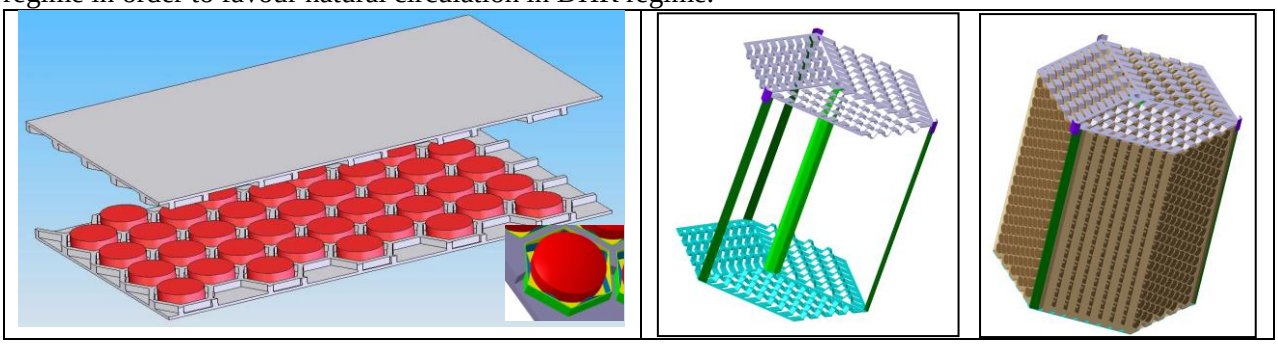

Fig. 3 Fuel assembly sketch

Considering the power density of the GFR core and its low thermal inertia, the decay heat removal relies on a gas circulation (natural circulation as far as possible) across the core but not on thermal inertia plus conduction/radiation.

Table 1 GFR2400 core main features

Core power (MWth)	2400
Core fissile height (m)	2.35
Core diameter (m)	3.8
Pu enrichment (%)	18.2
Delayed neutron fraction (pcm)	342
Doppler Constant (pcm)	-837
He depressurization ($), end of life at equibrium	0.9

In this paper, the calculation results presented for the GFR2400 are related to plate fuel type because more numerous study results were available for design extension conditions, but it is worth specifying that the same kind of trends have been obtained for pin-type fuel. A comparison between the two fuel element concepts is presented in (Malo et al., 2009) and have shown that the results presented here are can be extrapolated to a pin-type core design.

2.2 ASTRID reactor design (Sodium-cooled fast reactor, 1500 thermal megawatts)

ASTRID was designed to fulfil the Gen IV criteria in terms of safety, sustainability, economy and proliferation resistance (Le Coz et al., 2013). This reactor consists in a 1500 MWth SFR pool type reactor of about 600 MWe that is an integrated technology prototype designed for industrial-scale demonstration of 4th generation SFR safety and operation. Fuel type is oxide. The ASTRID pool type primary circuit includes 3 primary pumps and 4 intermediate heat exchangers (IHX) immersed in the reactor vessel (Fig. 4). Beyond a low void worth core design (CFV core), other innovative options have been investigated during the conceptual design period carried out between 2011 and 2015 in order to improve safety on the following points, for example: elimination of the possibility of sodium/water reaction at the interface between secondary loops and ternary circuit (investigation on the feasibility of a gas power conversion system instead of a water/steam system) (Bertrand et al., 2016) and enhancement of the reliability of the decay heat removal system (DHR) (Aubert et al., 2018). Each of the 4 secondary loops delivers a fourth of the core power (375 MWth) to sodium/gas heat exchangers. The gas power conversion system (PCS) uses nitrogen at 180 bars (turbine inlet) as the reference coolant. A Brayton cycle, which has never been implemented in any sodium reactor but has been investigated for High Temperature Reactors (HTR) has been chosen. This kind of cycle provides the best efficiency for a given gas heat source temperature (about 37% for ASTRID). An alternative design option operates with a steam/water Rankine PCS.

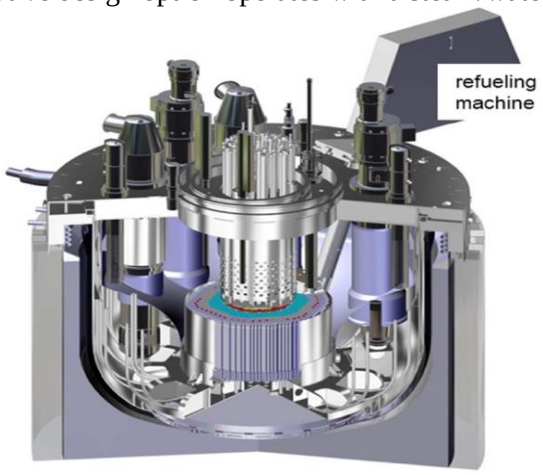

Fig. 4 Primary system arrangement for ASTRID

The version of the core investigated for ASTRID studies presented here is the CFV-v3 (core including mitigation devices, DCS-M-TT) whose features are detailed in Table 2 and Fig. 5. This core has been designed in order to increase the time before boiling in case of unprotected loss of flow (ULOF) accident and also to reduce the severity of a primary power excursion in case of severe accidents. For a classical core featured by a large positive sodium voiding effect, the sodium boiling transient resulting from a ULOF, would certainly lead to a large reactivity insertion that would cause a core power excursion (Papin, 2012). The low void worth effect of the CFV core results mainly from the presence of a sodium plenum above the fissile zones (Sciora et al., 2011) combined to the presence of a fertile plate in the inner core (Fig. 5). The height of the outer fissile zone enables the void reactivity effect to be decreased due to neutron leak enhancement. A previous comparison between a CFV core concept and a homogeneous core showed the better natural behavior[1] of the CFV concept before sodium boiling onset in case of ULOF (Chenaud et al.,

[1] Natural behavior: dynamic behavior of the reactor when the failure of all the systems designed to control a transient are assumed to be not actuated.

2013). The shroud of all the core sub-assemblies (SAs) represented on the right hand of Figure 5 consists in steel hexagonal tubes.

Table 2 ASTRID CFV-v3 core main features

Nominal thermal power [MW]	1,500
Inner fissile zone height (lower / upper) [cm]	25 / 35
Outer fissile zone height [cm]	90
Inner fertile zone height [cm]	20
Core diameter (m)	3.4
Fissile zones PuO_2 enrichment (Inner / Outer) [%vol.]	22.95 / 19.95
Effective delayed neutron fraction (β_{eff}) (pcm)	368
Doppler constant (pcm)	-963
Void reactivity effect ($), Core at equilibrium	- 0.5

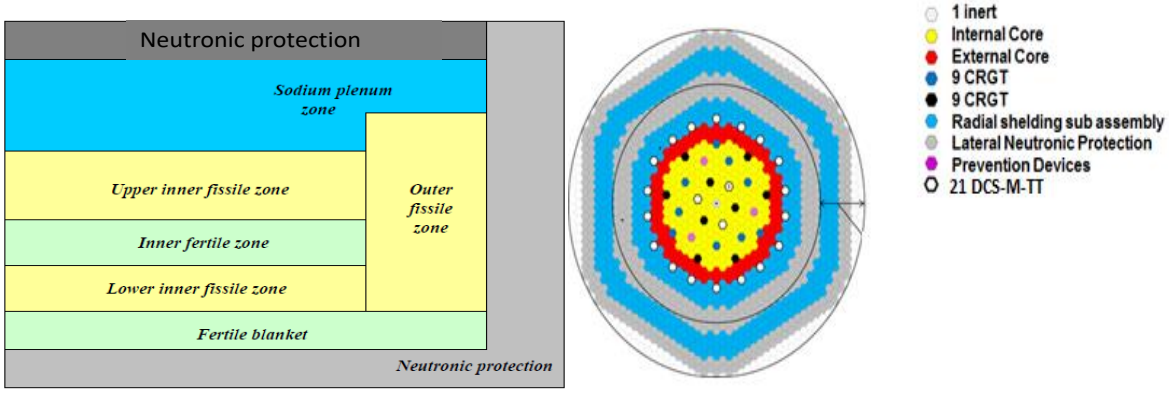

Figure 5. CFV general core geometry (left hand side: vertical cut; right hand side: horizontal cut). CRGT stands for control rod guide tube; DCS-M-TT stands for mitigation devices aiming at directly relocating the molten core materials on the core catcher)

Moreover, a core catcher is foreseen at the bottom of the main vessel in order to collect the core materials inside the primary vessel (Fig. 4). The aim of the core catcher is to spread the core materials in case of core meltdown to enable their cooling in a subcritical configuration and to protect the lower head of the vessel.

3. CROSS-COMPARISON OF CORE MELTING PREVENTION CAPABILITY FOR GFR AND SFR

The main transient families able to lead to core melting are first presented in this section since their study enables to show the core melting prevention capability of the concept. Then the most challenging situations are discussed for the GFR and for the SFR. It is worth noticing that both concepts are designed to withstand all design basis accidents combined with an aggravating failure that should be adopted in the classical deterministic safety approach. Therefore, the article is voluntarily focused on challenging situations and transients beyond the design domain in order to tackle some core evolutions and some physical phenomena that are very hypothetic but that could lead to very degraded reactor conditions that could lead to radiological releases. In this sense, most of the challenging transients are unprotected (SFR and GFR) or associated to depressurization of primary circuit (typical of reactors under pressure like GFR).

3.1. Main relevant accident sequences for prevention study

For the two considered concepts, the core materials melting can be obtained if the ratio between the core produced power P (W) and the power extracted from the core Q (W) is too low to prevent the core material from heating up to their phase change temperature. Finally some initiating events lead directly to reactivity insertions and their resulting transients are called transient overpower (TOP or UTOP in their unprotected versions). The heat extracted from the core Q can be very roughly expressed as:

$$Q = \dot{m}\, C_p (T_{out} - T_{in}) \qquad (1)$$

Where $\dot{m}$ is the core flow rate, C_P the coolant heat capacity and T_{out} and T_{in} are respectively the core inlet and core outlet temperatures. Equation (1) enables to make a relation with the main transient family leading to reduce the heat extraction from the core Q that occurs in case of:

-loss of or decrease of primary flow rate $\dot{\mathbf{m}}$ called (LOFA and LOCA for the GFR[2]);
-loss of secondary side that is called loss of heat sink (LOHS) that leads to lower **Q** because of $\mathbf{T_{in}}$ increase ;
-loss of power supply (external (LOOP) or total (TLOP)) that leads to a decrease of the primary flow by a loss of active systems and to a partial or total loss of heat sink and of secondary side flow rate; such events leads to a combination of the two previous effects.

Finally, some local loss of flow (SA fault, SAF) can occur at the SA scale and its bounding case in terms of magnitude and dynamics is discussed for both reactor concepts. The calculated sequence events do all belong to beyond design situations since both reactors have been designed to withstand design basis accidents (DBAs) without core melting ((Bertrand et al., 2016) and (Bertrand et al., 2008)).

3.2. GFR2400 prevention capability in case of very challenging situations

Considering the low density of helium (light gas) and its low thermal conductivity (good for a gas but low compared to that of liquid metals), the power density of the GFR 2400 that is close to that of a PWR (Bertrand et al., 2020) and the small coolant mass included into the reactor, the core melting prevention relies on convection with a gas circulation into the core. Thus, the GFR2400 DHR strategy relies on the actuation of various systems depending on the pressure and on the core power level (Fig 6). The selected combination of systems takes into account the two main accidental situation families: the pressurized situations (intact primary boundary) and the depressurization situations resulting from a LOCA. In addition, the situation related to a primary pressure reaching around 0.1 MPa, corresponding to a combination of LOCA and a leak of the CC, has been considered. Such an architecture of the DHR system has been assessed with a line of protection approach (Bertrand et al., 2009) and satisfies its requirements, in particular, thanks to the natural convection capability in case of small breaks. It is worth noticing that the DHR operation based on natural circulation with a heavy gas for small breaks relies on the presence of the CC insuring a back-up pressure of about 1 MPa. This CC permits also to design DHR blowers with a low pumping power, compatible with an emergency electrical power supply, delivered by Diesel engines. Moreover, as indicated be Bertrand (2012), in case of particularly frequent situations able to affect the water feeding system or the off-site power or unprotected transients, the PCS can be used to cool the core.

3.2.1. Core melting prevention criteria

[2] In case of LOCA, the pressure decreases and so the density. As a result, the primary mass flow rate being proportional to the density, the flow decreases as well in case of LOCA (like for a LOFA).

All the acceptance criteria below have to be fulfilled in order to prevent a severe accident. Actually, they are those of category 4 situations:

- fuel temperature < 2000°C ;
- clad temperature < 1600°C or < 2000°C during a short time ;
- no degradation of the fluid channel able to prevent the core cooling.

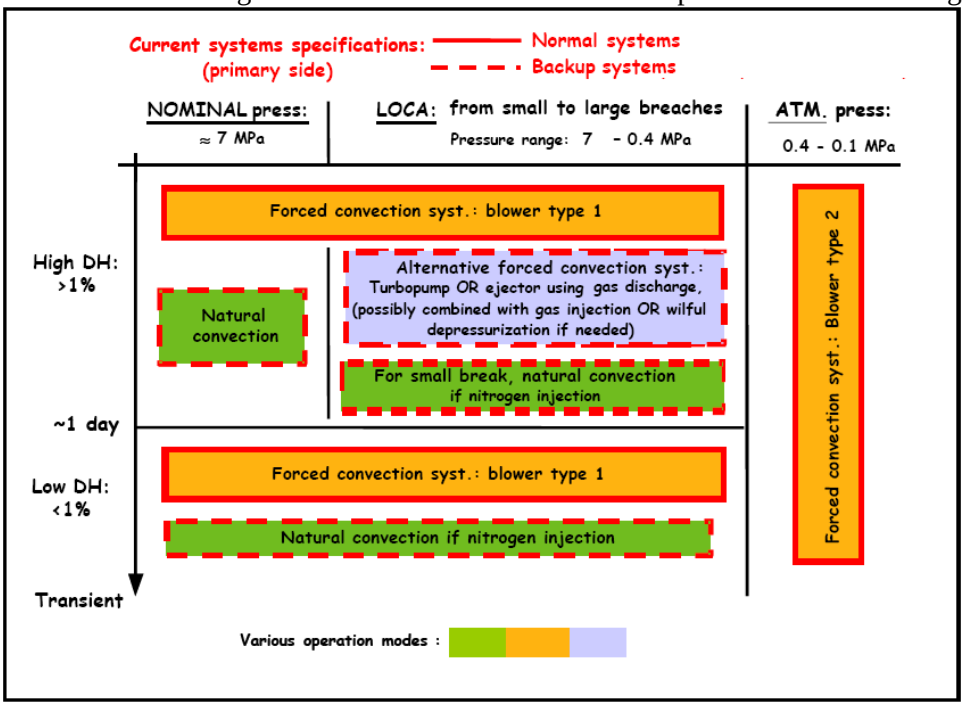

Fig. 6 Sketch of the DHR operation (DH: decay heat): y-axis values decreases with decay-heat after reactor scram and x-axis values are related to pressure range depending on the considered transient

3.2.2. Protected challenging transient

Basically, as long as the primary circuit remains under pressure and as soon as the reactor shutdown is actuated, the peak cladding temperature (PCT) fulfills largely the acceptance criteria (Bertrand et al., 2008). Thus only prevention capability in case of various depressurization situations are presented in this section. All the transients whose results are presented in Table 3 are beyond design basis accidents (BDBAs) since all the initiating events correspond to the bounding large break LOCA (class 4 event) combined with additional failures. The 55 inch break corresponds to the whole cold duct equivalent section. The CATHARE2 modelling is presented for instance by Bentivoglio (2009) and will not be further detailed here. The acceptance criteria are only fulfilled if enough flow rate can cool the core after the depressurization and if the flow rate is sufficient during the main depressurization in order to limit the PCT of the transient. In all the transient combined with the failure of active means, the only way to limit the heating and to shorten the peak is the accumulator discharge (Fig 7). This latter Figure shows the core and upper plenum temperature evolutions on its left hand side as well as the core flow rate. As it can be seen on this evolution, the drastic flow rate decrease occuring at the beginning of the transient, that is, before accumulator discharge leads to a temperature increase stopped after 1000 seconds. The right hand side of Figure 7 presents the pressure evolutions in the primary circuit, in the accumulator and in the close containment. A comparison of the both sides of Figure 7 illustrates that the core flow rate is directly related to the primary flow rate. Finally, one can see that when the accumulator pressure is balanced with the CC pressure the nitrogen discharge is over. The large break LOCAs cumulating a large break in the CC (full depressurization) leads to fuel element degradation if the accumulator discharge is not actuated. This kind of transient leads to a PCT higher than the acceptance criteria if active DHR operating mode is not available.

When this mode is actuated, since the pressure in the primary circuit is rather low, only one DHR loop is actuated otherwise a surge regime would affect the blower operation. However, in case of integrity of the CC, nitrogen injection would enable to prevent core melting if one active DHR system is available. Moreover, Figure 7 indicates that, providing that the CC keeps its leaktightness, the core can be cooled in natural circulation without exceeding fuel/cladding liquefaction temperature (see section 4 for further details). As a conclusion, calculations presented here indicate that the DHR strategy necessary to manage the challenging situations of fast (and sometimes almost total) depressurization of the primary circuit is complex and requires several active systems combined with nitrogen injection or an additional system able to operate around atmospheric pressure (named blower type 2 in Figure 6). Nevertheless, the conclusions written here on core degradation prevention for very specifically selected challenging situations have to be nuanced by the results provided by Bassi (2010) showing that the core melting frequency (reactor state at nominal power) is acceptable, that is, near that of generation 3 reactors.

Table 3 Behaviour of the GFR 2400 in case of core melting prevention situations (FC: DHR loop in forced convection; NC: DHR loops in natural circulation; v = 30 000 m^3 corresponds to a sensitivity study to the containment building)

Primary break size (inch)	Downcomer flow rate at PCT (kg/s)	Tmax Claddings (°C)	Accumulator injection	Pressure max in CC (bar)	CC break size (inch)	Pressure in CB (bar)
55	25 (3 loops FC)	1570	no	9,5	-	1
10	58 (2 loops NC)	1800	yes	13	-	1
10	7,3 (1 loop FC)	> 2500	no	6,6	10	1,65
10	9,5 (1 loop FC)	2030	no	7,1	10	2 V=30000m^3
10	8,7 (1 loop FC)	1280	no	7,8	2	1,65
10	90 (1 loop FC)	730	yes	7,1	10	3

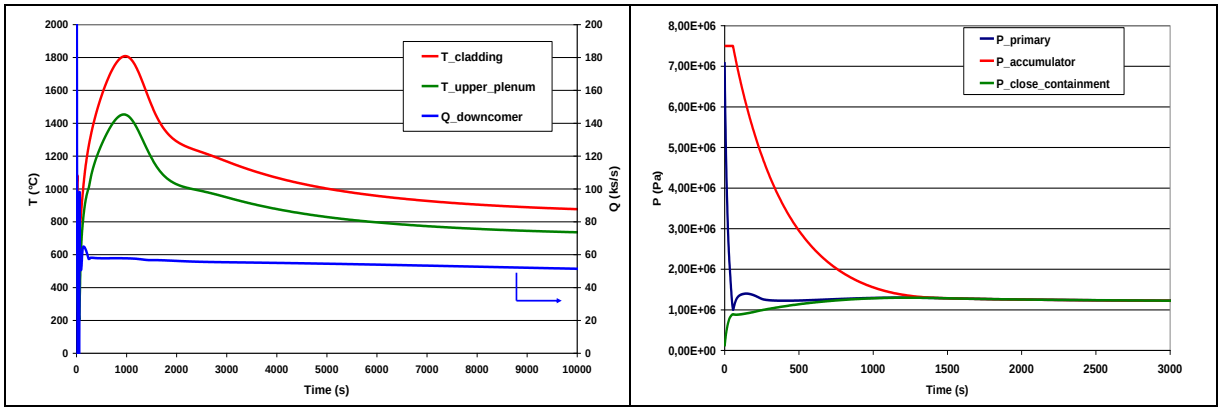

Fig. 7 Temperature, pressure and flow rate transient resulting from a 10 inch LOCA controlled in natural circulation thanks to nitrogen injection (3 accumulators)

3.2.3. Unprotected transients

UTOPs, ULOFAs and ULOCAs have been investigated in order to assess the capability of the GFR2400 to prevent core melting. Regarding UTOP, control rod assembly (CRA) ejection being prevented by design (Malo et al., 2008), the full withdrawal of a single CRA has been investigated. Whatever the velocity of the rod extraction, it does not lead to exceed a PCT of about 1100°C the asymptotic power being equal to about 3000 MWth (Girardin, 2009). ULOFAs can be managed in order to prevent fuel SA degradation thanks to the use of pony motors powered by emergency electrical power supply and of steam generator power extraction (Fig. 8). More in detail, as it can be seen in Figure 8, the main contribution to the core reactivity

decrease leading to core power decrease during the 100 first seconds of transient, is the Doppler reactivity feed-back. The only small positive contribution results from the coolant heating that decreases its density. After 200 seconds, the core power is stabilized to 500 MW that is still a high power value. ULOCAs cannot be managed without core damages and consists in core melting sequence initiators as indicated in Figure 9 for the bounding SB-LOCA. Therefore, their consequences will be analyzed in section 4. However, thanks to a dedicated management of the accident by increasing of 20% the primary blower speed, the alternator disconnection from the grid and by depressurizing the SGs (Bertrand et al., 2010) in order to have a more heat extraction by water vaporization, some delay up to core melting can be gained, thus delaying the fuel degradation of more than one hour. However despite this enhancement of the heat sink power extraction and of the primary flow rate thanks to nitrogen injection and to speed blower increase, the core power remains very high (around 1000 MW). On the one hand, enough flow is needed to cool the core, but on the other hand, the nitrogen injection enabling to keep a large flow rate has a bad impact on the core reactivity because its depressurization effect is less favorable than that of helium. As a result, after nitrogen injection in the primary circuit, this gas is released to the primary circuit breach, the pressure decreases and the power is stabilized at a high level at the end of the depressurization.

3.2.4. Conclusions on core melting prevention for GFR2400

The results presented in the previous sub-sections indicate that in case of pressurized transient and of UTOPs, the prevention capabilities of the GFR2400 are rather good. Conversely, the studies presented here have confirmed the difficulty to cool the core in case of LOCAs combined with a failure of the CC. The ULOFAs can be managed thanks to primary flow rate back-up and to the heat removal by the PCS. ULOCAs lead to core degradation even if its dynamics could be reduced by implementing a dedicated complex piloting procedure of the reactor.

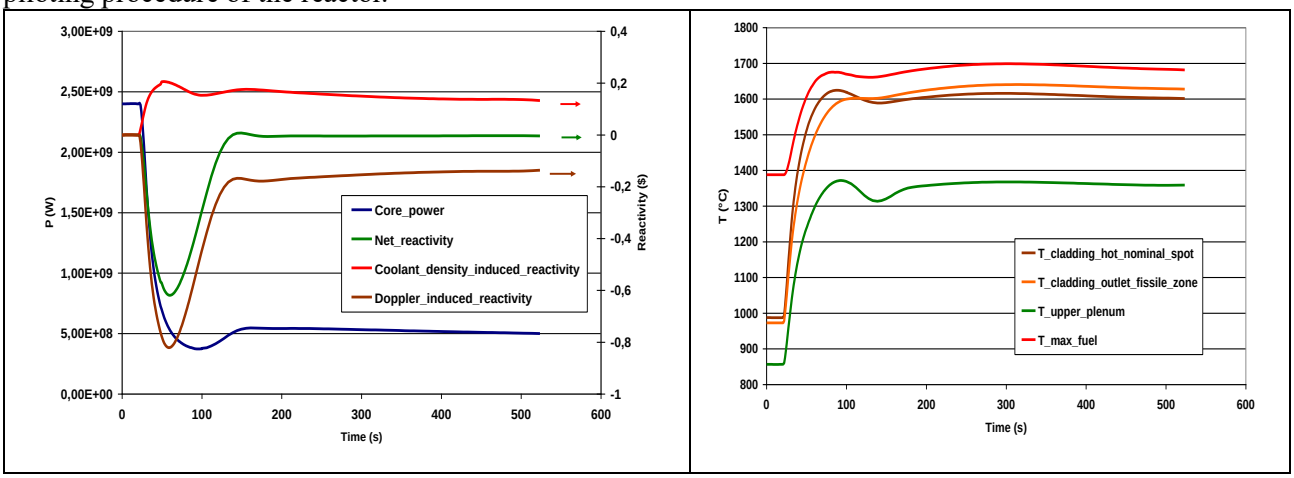

Figure 8 Unprotected loss of flow (ULOFA): core power evolution and reactivity balance (left side); core temperature evolution

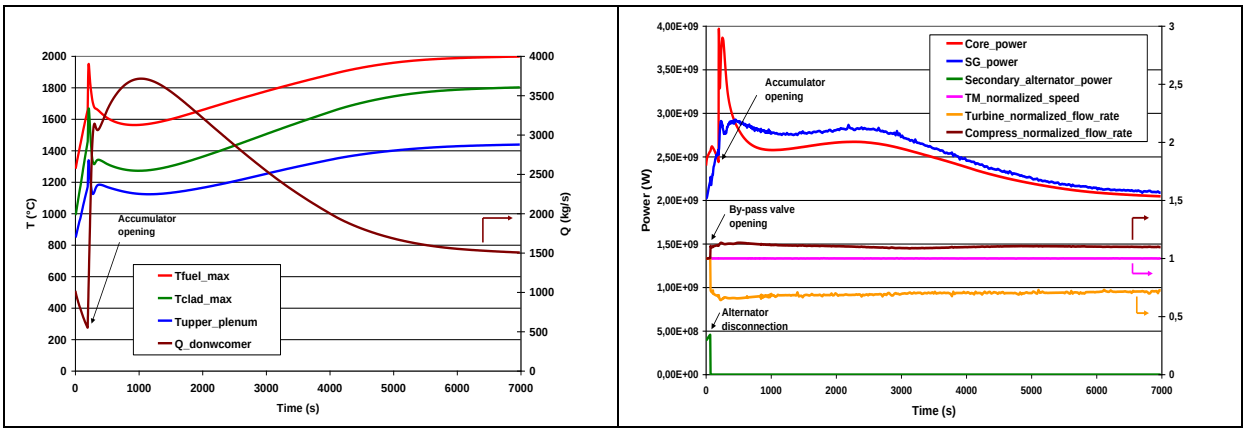

Figure 9 Transient behaviour of the GFR in case of 3 inches unprotected SB-LOCA (enhancement of cooling by increasing the speed of the primary blowers and SG operating adaptation)

3.3. ASTRID core prevention capability in case of very challenging situations

The simplified assessment provided by Bertrand (2021) have shown that pool type SFR concepts have a large thermal inertia provided by the coolant mass and a large margin to coolant boiling as soon as the reactor scram has been actuated. Therefore, generally speaking, protected transients are not a big issue for SFRs compared to GFRs in terms of core melting prevention. However, the sodium should not be heated too much in order to protect the reactor vessel and the redundancy and diversification level of system removing the decay heat should be adequate as shown by Aubert (2018). Having considered that, the protected transients do not consist in very challenging situations for SFRs. So they will not be presented in this section.

3.3.1. Core melting prevention criteria

The decoupling criteria ensuring that no core melting will occur are the following ones:

-maximum sodium temperature lower than its saturation temperature;
-PCT lower than 825 °C;
-hexcan maximum temperature lower than 800 °C;
-Fuel melting fraction lower than 5% in a pin.

The two first criteria are aimed at avoiding the core draining from its sodium. The third one enables the core to keep its overall geometry by avoiding hexcan failure and the last one prevents channel fuel ejection in case of TOP.

3.3.2. SFR core melting prevention in challenging situations

Among the three sequence families able to lead to a whole core melting situation, the local cooling fault (SAF) and the TOP induced by a control rod withdrawal (CRW) will not be addressed here since their consequences depend on accident detection. In other terms, if the local event is detected on time, the core melting is prevented with a comfortable margin. Thanks to the favorable reactivity feed-back (mainly Doppler feed-back) and to the limited reactivity swing of the CFV core, whole core melting is prevented even in case of CRW without scram. Conversely, an unprotected sub-assembly fault (USAF) leading to a whole SA flow blockage would propagate to a large part of the core if the accident is not detected but its consequences are covered by the study of degraded states presented in section 4. So, in order to compare prevention capability between ASTRID and the GFR2400, a ULOFA has been calculated with the reference gas PCS and for a classical steam/water PCS as well. Simulations were performed with the CATHARE2

code and more details are provided by Droin (2020).

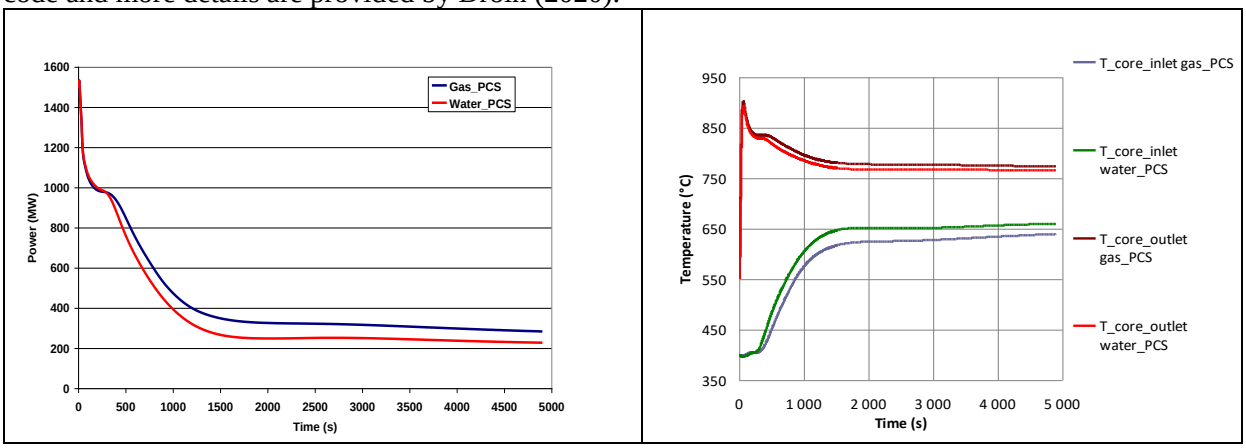

Figure 10 Core power evolution in case of unprotected LOOP (with gas PCS option and with water steam PCS option) (Bertrand et al., 2016a)

The loss of off-site power (LOOP) can be managed without scram. The power (Fig. 10), governed by the reactivity feed-back (Droin et al., 2020) decreases enough to prevent sodium boiling and core degradation. However, the primary vessel being at a temperature causing thermal creep, it would be necessary to decrease the core power after the first temperature peak in order to avoid primary vessel failure. If Figure 10 indicates that the sodium temperature remains too high in case of ULOFA, it has been shown (Aubert et al., 2018) that if the PCS is shut down, the sodium asymptotic temperature is less than 700°C because the reactivity feedbacks are more favorable without PCS operation. This vessel temperature value provides a longer grace delay in order to later scram the core before having a significant risk to jeopardize the main vessel. Moreover, a large number of ULOFA sequences caused by an unprotected station black-out (UTLOP) have been performed by a CEA house fast-running software called MACARENa (Droin et al., 2020). Calculations have shown (Fig. 11) that by varying the initial reactor conditions and by propagating uncertainties on the lack of knowledge in the models, in 75% of the sequences the core melting is avoided, either because no boiling occurs, either because the boiling is stabilized and does not propagate in the fissile region of the core. This result is quite satisfactory for a SFR because with a classical core with a positive overall void worth, a ULOFA without any back-up flow rate leads to a core melting resulting from a power excursion. For ASTRID, in a quarter of the sequences, this ULOFA consists in a core melting initiator. It should be noticed that the core melting prevention capability has been increased in the ASTRID actual design by including into the core some passive shutdown device systems (Marie et al., 2021). Finally, the TOPs can induce core melting as soon as they are due to large scale events but most of this kind of events can be prevented by specific design provisions (gas bubble ingress surveillance and prevention into the primary coolant, core support failure prevention by structure diversification, core devices preventing SA compactions). Nevertheless, no matter the initiating event, the consequences of reactivity insertion ramps have been investigated and are presented in section 4.

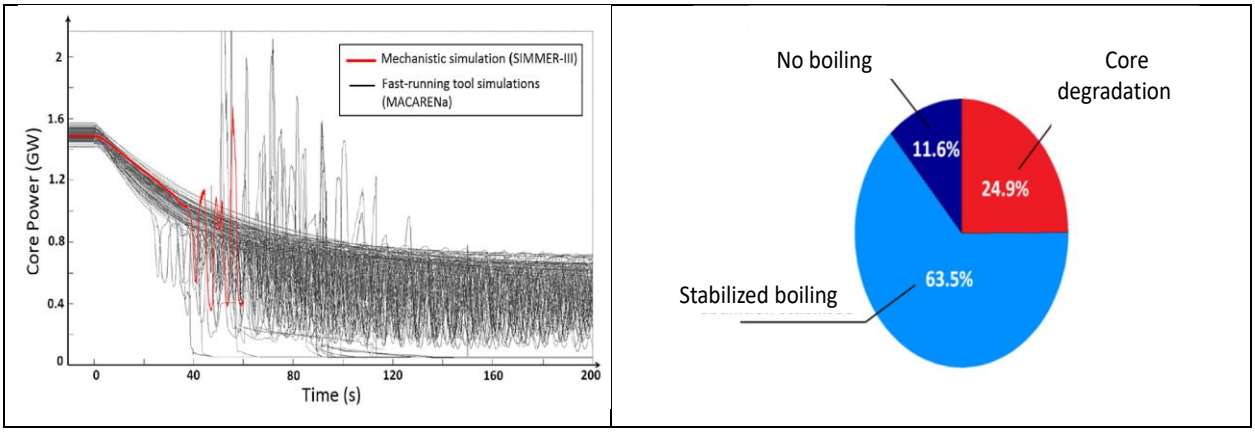

Figure 11 Core power evolution in case of unprotected station black-out (SBO) and fraction of core melting prevention and of core melting situations (Droin et al., 2020)

3.3.3. Conclusions on core melting prevention for ASTRID

The core melting capability on pool-type SFRs and especially on ASTRID is rather good thanks to the large sodium inertia of the primary vessel and to the large margin up to sodium boiling (Bertrand et al., 2021) as soon as the reactor shutdown is successful. The core melting prevention in case of local faults relies mainly on accident detection on time and then on reactor shutdown actuation. Finally, some UTOPs and ULOFAs of very low frequency, called mitigation situations can initiate core melting and the study of their consequences is presented in section 4.

4. CROSS-COMPARISON OF CORE MELTING MITIGATION FOR GFR AND SFR

Challenging situations able to lead to core melting have been presented in the previous section both for GFR and SFR. In this section, a cross-comparison is proposed once the core degradation has started. In section 4.1, a brief presentation of the various severe accident phases of a fast neutron reactor is presented whereas in section 4.2, some insights regarding the core degradation process and its associated effects on core power are presented. Finally, the possibility to have some mechanical consequences on the reactor vessel is discussed and compared for both concepts.

4.1. Fast neutron reactor severe accident scenarios

Due to the large enrichment in plutonium their cores (about 20 %), fast neutron cores do not operate in their most critical configuration. Thus, core melting or coolant voiding tends to increase the reactivity and the core power. This features are the same for a 2400MWth (GFR2400) and a 1500 MWth (ASTRID). Both concept have to deal with large cores. So it means that in case of unprotected transients, the accident is largely governed by the coupling of materials movements with the reactivity. Basically, a severe accident scenario gathers the following phases:

- the primary phase during which the movements of the materials are predominantly axial and which begins at the initiation of the degradation of the fuel pins and ends at the first ruptures of the hexagonal tubes (HT);
- the transition phase which corresponds to the loss of integrity of the HTs, resulting either from their melting or from the loss of their mechanical integrity. During this phase takes place a transition between the axial relocation and the radial propagation of the degraded materials;
- the secondary phase during which the degraded core forms one or more large molten pools (cases of the CFV core), which may induce re-criticalities;

- the post-accidental cooling phase during which a large part of the core material inventory is located on the core catcher.

It is also referred to the expansion phase: this is the phase of the accident during which liquid materials suddenly vaporize and then expand, producing mechanical work. The expansion phase can occur when a power excursion affects the core. The nature of the families of sequences has a decisive influence on the primary phase, whereas during the secondary phase it is possible to describe the accident evolution by starting from several core degraded states that are relatively independent of the previous evolution of the scenario. Therefore, those degraded states are pretty generic and result of most of the scenario evolutions taking place during primary and transition phases (Bertrand et al., 2016b) The primary phase of the accident can result from families of sequences of section 3 that lead to core melting. As far as degraded states are concerned, some generic effects on reactivity and mechanical loadings will be considered in this section.

4.2. GFR severe accidents

During the primary phase of accidents, the core degradation can be initiated by chemical reactions caused by fluid ingress in the primary circuit (water/steam, nitrogen or air). This kind of effects, presented by (Bertrand et al., 2012) will not be detailed here since we will be focused in core material heating induced by major challenging situations. Considering the liquefaction temperature of the fuel SAs system (UPuC/W-Re-SiC multi-layer system) and the chemical interaction taking place before liquefaction, core degradation is largely governed by physical-chemistry interactions. Indeed, the W-Re can be consumed on each of its face by solid phase interaction with the fuel pellet and the cladding and a liquid phase appears at about 1900°C on its inner face and at about 1850°C on its outer face. The core materials being refractory, the fuel starts to melt at 2200°C and the cladding and the liner start to decompose at about 2700°C (Bertrand et al., 2012). In case of direct contact between cladding and fuel, a liquid phase is present if the temperature of the materials is higher than 1600°C. Before the material relocations, reactivity effects during the primary phase of core melting sequences are very limited and cannot induce a large power excursion because the Doppler integral is larger than the void worth coefficient. Thus, this latter is not able in itself to cause prompt-criticality because it is lower than the delayed neutron fraction (Table 1). Reactivity effects that could be obtained in transition and secondary phases have been assessed (Bertrand et al., 2010) and have shown that the reactivity inserted by core melting (material compaction by formation of a molten pool) exceeds 1 $ for segregated core materials as soon as 7 SAs are molten. However, no transient calculations of such a core degradation in secondary phase exists yet for the GFR2400. Finally, an interested point deals with the possibility to release mechanical energy in case of large reactivity insertion into the GFR core. This release could be due to fast phase change because of the sudden vapor formation at high pressure and their subsequent work transmitted to the primary vessel. The higher the temperature, the higher the pressure of the vaporized materials. Thermodynamic equilibrium calculations have shown (Bertrand et al., 2012) that the Si resulting from the decomposition of the SiC would be the main contributor of the total vapor pressure in case of vaporization of the core materials at a high temperature (this pressure exceeds 1 bar above 3000°C and reaches 100 bar around 5000°C). The core degradation process during the primary phase of a bounding SB-ULOCA presented on Figure 9 has been investigated by chaining the CATHARE2 temperature evolution in the core with a modelling of the physico-chemical interactions (Figure 12). On the cladding side, at 7500 s, the totality of the liner has been consumed at the hot spot of the core only by the liner/cladding interaction occurring in solid phase. By considering the degradation of the liner from both sides, it has been fully consumed after 2 hours when it is not liquefied before in its inner face. As a conclusion, the strategy proposed to control the bounding unprotected SB-ULOCA enables to shutdown the reactor within a time period ranging from 1.5 to 2 hours after the accident without any loss of a coolable geometry of the core.

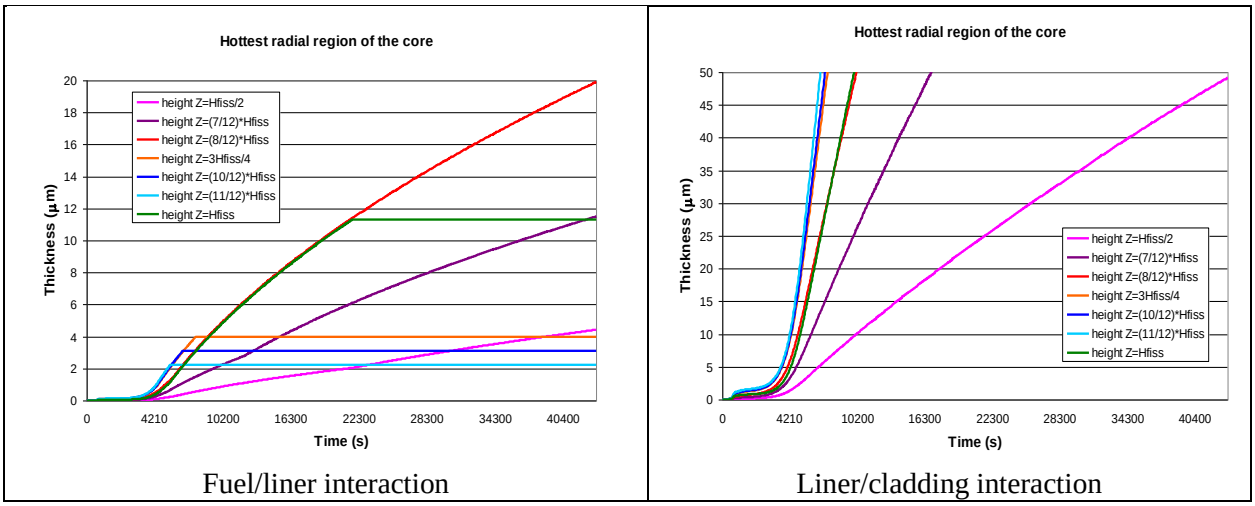

Fig. 12. Thickness of liner consumed versus time in case of a bounding SB-ULOCA in the hottest region of the core (horizontal plateau means the reach of liquefaction)

Let us now consider a large core degradation supposed to be spatially coherent no matter the initiating event, thus leading to a large axial compaction of the core materials due to their relocation triggering a power excursion. Such a large core degradation could be quite generic, or could be induced by a LB-ULOCA and therefore, the pressure preceding the power excursion has been supposed to be around 5 bars (back-up pressure of the CC). Assuming a very rough modelling of the power evolution thanks to a single neutron group, the power evolution following a postulated reactivity insertion around 2 $ has been considered (Bertrand et al., 2012). The approximated pressure peak following the material phase change does actually not exceed the nominal pressure of the vessel according to our approximate calculation and is close to 20 bars. Then, by considering equation (2), one can calculate the mechanical energy when expanding the gases up to the atmospheric pressure, where V (m^3) and P (Pa) are the volume and the pressure and where the indices i and f refer respectively to the initial state and the final state of the gas. γ is the ratio of the heat capacities of the gas considered here as monoatomic. For example, according to equation 2, for a pressure Pi of 20 bars, the expansion of the vaporized materials from half of the compacted core[3] (Vi close to 6 m^3) to a pressure of 1 bar would produce a work of about 13 MJ.

$$E_{meca} = (P_f V_f - P_i V_i) / (\gamma - 1) \quad (2)$$

This value is very small, in order of magnitude, compared to the mechanical energy that could affect a SFR because the sodium vapor pressure is much more higher than that of the GFR core materials. The advantage for the GFR is that the pressure build-up is not so high as in SFRs because there is no FCI (the gas coolant does not contribute to the pressure build-up).

4.3. SFR severe accidents

One of the main design objectives of the CFV core is to optimize its natural behavior in order to avoid energetic power excursions that occur during the primary phase of a severe accident for a classical large SFR core (Papin, 2012). Thus, in case of ULOFA, owing to the sodium voiding effect, the transient leads either to a coolable state of the core, by stabilizing the boiling or by establishing a natural monophasic convection regime, either to a non coolable state (Fig 11) of interest in this section. If the boiling of sodium

[3] Such a degraded core state enables to study its consequences without considering a too specific scenario. It enables to cover unknown or forgotten scenarios by being not too scenario-dependant.

in the plenum of the hottest SAs occurs, this leads to a decrease of the core power due to negative reactivity insertion when voiding the plenum (Bertrand et al., 2018). When the boiling front penetrates into the positive void worth region of the core, the power ceases to fall, or rises slightly, causing the sodium to boil in the plenum of other SAs and again, the power decreases. Thus, in spite of power oscillations linked to the boiling transient into the core, the power gradually decreases. Consequently, the degradation of dried fuel rods takes place at low power by degradation of the clads and then of the fuel pellets. Therefore, due to the natural behavior of the CFV core preventing a large power deposition during the primary phase of an ULOFA, it is very unlikely to have a large mechanical energy release. Furthermore, the ASTRID core is designed to prevent significant reactivity insertions: space between HTs as low as possible in nominal operation (minimal compactness of the core), limitation of gas sources, piloting of the core power with all the control rods. Despite the UTOP prevention measures mentioned before, they have been considered to occur in order to assess the core behavior. So parametric studies of postulated reactivity insertion ramps indicate (Bertrand et al., 2016b) that the CFV core leads, in the primary phase, to a lower mechanical energy release by expansion of the fuel vapor than a homogeneous core.

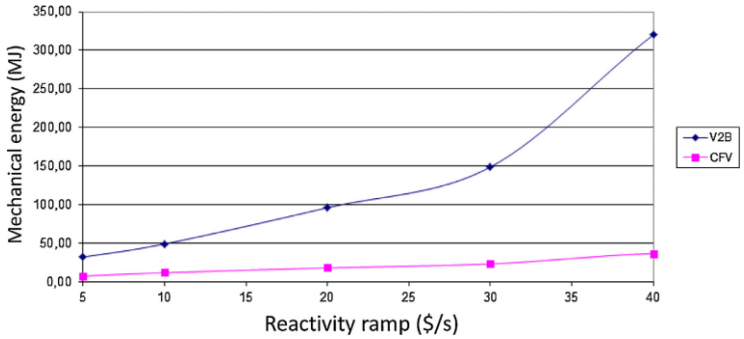

Fig. 13. Mechanical energy release for postulated UTOPs (ramps between 5 and 40 $/s), based on fuel vapor expansion, for a classical homogeneous core (V2B) and the current ASTRID core (CFV)

The behavior of the CFV core during the transition and the secondary phases has been investigated thanks to three successive steps: inventory of the reactivity effects able to trigger power excursions when the core has lost its geometry (static study of the impact of each reactivity contributor), study of scenarios by starting from generic degraded states (investigation of the whole range of reactivity possible insertions) and finally verification of trends obtained by degraded state studies through investigation of accident scenarios by starting from the nominal state of the reactor. Static calculations performed with ERANOS for a degraded state with the inner core molten (Fig 5 and (Bertrand et al., 2016b)) have shown that dominant effects on the reactivity evolution are related to:

- Axial compaction of the inner core: ~ 14 $;
- steel decantation from the molten zones: ~ 7 $;
- fissile material extraction from the degraded zone ~ - 0.25 $/(mass percent).

By putting into play those reactivity effects, the thermal energy deposited in the fuel before its vaporization and expansion, the mechanical energy that would be released by the isentropic expansion of the fuel vapor is about 100 MJ (Bertrand et al., 2018). In addition to these parametric analytical calculations performed for identification of mitigation provisions needs and for investigation of the range of expected mechanical energy, ULOFA scenario calculations performed with SIMMER III (Kondo et al., 2000) from the nominal reactor state have shown (Fig 14) that the core natural behavior (no DCS-M-TT) is featured by two power excursions during the secondary phase because the fissile materials are not ejected in a large enough amount from the core after the first power excursion to prevent further recriticality. As a result, the thermal energy deposited in the fuel during these power excursions leads to superheat a significant fraction of fuel inventory up to 4500 K. The expansion of this fuel calculated without taking into account the energy absorption in

the core surrounding structures would lead to a mechanical energy of an order of magnitude of 100 MJ (Bertrand et al., 2018). Considering this possible energy release, even if it is low compared to that of former project (Superphenix vessel design energy was 800 MJ), some mitigation tubes (DCS-M-TT) have been integrated into ASTRID core in order to discharge the molten fuel from the neutron flux and to limit power excursion occurrence and magnitude. Thanks to the DCS-M-TTs, the mechanical energy release is of about 10 MJ for the power transient plotted in Figure 14.

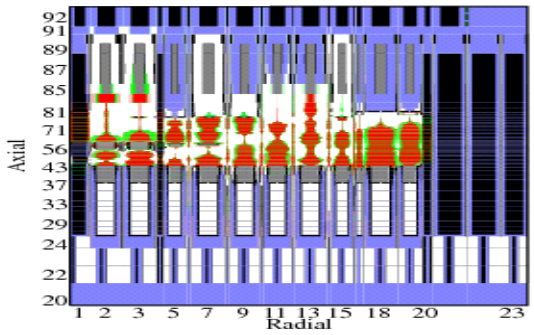

Core state after secondary power excursion (no DCS-M-TT)

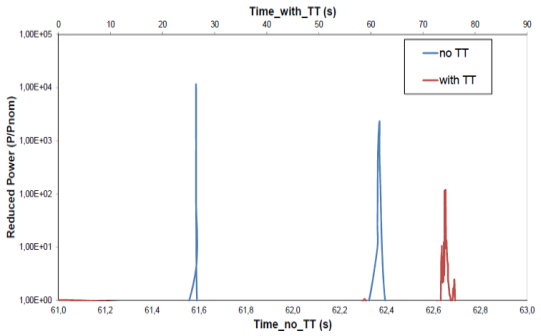

Normalized power evolution during secondary phase with and without DCS-M-TTs (time zoom on power increase)

Fig. 14. Core state after first power peak (left hand side) and normalized power evolution without and with mitigation devices (right hand side) for ULOF whole scenario calculation

5. CONCLUSIONS

A synthetic cross-comparison of core melting prevention and core melting mitigation capabilities have been performed for GFR and SFR on the basis of more detailed papers referenced in the present paper. As a result, the elements presented here have been chosen on this purpose among studies carried-out from 2007 to 2016 on the GFR2400 and ASTRID reactors developed at CEA. This work is aimed at stepping back in order to catch trends on accidental behavior on Gen IV concepts of comparable large power depending on their preliminary design. Such an approach should help to think about future reactor designs by better knowing their advantages and drawbacks. Regarding prevention in case of very challenging situations, the main results of CEA accident analysis, have shown that the GFR concept cannot withstand full depressurization and unprotected transients because there are less favorable reactivity feed-back in GFR than in SFR. As a result, the ratio power/flow rate is too high to prevent core degradation, even in case of a back-up flow rate. The protected transient of SFR are easily managed and the unprotected one would lead to core melting only in case of some unfavorable aggravating events (like failure of emergency power supply) or in case of very unlikely UTOPs that should be prevented by design (large gas bubble crossing the core or core compaction). Regarding core melting situations, the primary phase of the accident is not able to induce mechanical energy release in the GFR2400 case due to the absence of volatile materials into the core, neither for ASTRID thanks to its low void worth core. However regarding ASTRID, the possibility to have an energetic FCI in the SAs induced by out-pin fuel ejection in case of fast UTOP should still be investigated carefully in order to consolidate the studies. Regarding the secondary phase, GFR core materials being less volatile than steel and sodium, the possibility to generate mechanical energy is low. This possibility is taken into account in ASTRID by adding mitigation tubes into the core whose aim is to discharge the fuel from the core as early as possible to reduce its reactivity. However, in the absence of sodium, the cooling of GFR degraded core materials would not be possible in-vessel and these materials should be spread and cooled in the close containment of the reactor. This close containment consists in an additional physical barrier mitigating fission product (FP) release, mitigation that is very efficient for SFR thanks to sodium. Finally, we can keep in mind that core melting prevention capability is low for GFR compared to SFR and that GFR is less likely than a classical SFR (with positive voiding core and no

mitigation tubes) to release mechanical energy in case of severe accident. The FP retention capability and post-accident cooling phase, which are very good in SFR are still to be investigated for GFR.

REFERENCES

Bertrand F., Marie N., Bachrata A., Droin J.B., Manchon X., Le Meute T., Merle E., Heuer D., Simplified criteria for a comparison of the accidental behaviour of Gen IV nuclear reactors and of PWRS, Nuclear Engineering and Design, 372, 2021, 110962

Malo, J. Y., Alpy, N., Bertrand, F., Cadiou, T., Chauvin, N., Dumaz, P., Haubensack, D., Geffraye, G., Jonqueres, N., Lorenzo, D., Morin, F., Nicolas, L., Peneliau, Y., Ravenet, A., Richard, P., Studer, E., Gas cooled fast reactor 2400 MWth, end of the preliminary viability phase, International Conference on Advances in Nuclear Power Plants, ICAPP 2008, Volume 1, Pages 208-218, 2008

Malo, J.Y. et al., Gas Cooled Fast Reactor 2400 MWTh, status on the conceptual design studies and preliminary safety analysis, ICAPP 2009, Tokyo, Japan, 10-14 May 2009

Le Coz P., Sauvage J.F., Hamy J.M, Jourdain V., Biaudis J.P, Oota H., Chauveau T., Audouin P., Robertson D., Gefflot R., The ASTRID Project: status and future prospects, proceedings of FR13, Paris France 4-7 March 2013, Paper CN 199-261, 2013

Bertrand F., Mauger G., Bensalah M., Gauthé P., Transient behaviour of ASTRID with a gas power conversion system, Nuclear engineering and design, Volume 308, November 2016a, Pages 20-29

Aubert F., Baude B., Gauthé P., Marquès M., Pérot N., Bertrand F., Vaglio-Gaudard C., Rychkov V., Balmain M., Implementation of probabilistic assessments to support the ASTRID Decay Heat Removal systems design process, Nuclear Engineering and Design Journal, Volume 340, December 2018, Pages 405-413

Papin J., Behavior of Fast Reactor Fuel During Transient and Accident Conditions, Comprehensive Nuclear Materials 2nd edition, Volume 2 doi:10.1016/B978-0-08-102865-0.00039-X 339, 2012, Elsevier Ltd

Sciora P., Blanchet D., Buiron L., Fontaine B., Vanier M., Varaine F., Venard C., Massara S., Scholer A.C., Verrier D., Low void effect core design applied on 2400 MWth SFR reactor, proceedings of ICAPP 2011, Nice, France

Chenaud M.S., Devictor N., Mignot G., Varaine F., Vénard C., Martin L., Phelip M., Lorenzo D., Serre F., Bertrand F., Alpy N., Le Flem M., Gavoille P., Lavastre R., Richard P., Verrier D., and Schmidt D., Status of the ASTRID core at the end of the preconceptual design phase 1, Nov 2013 · Journal of Nuclear Engineering and Technology, VOL.45 NO.6 NOVEMBER 2013, http://dx.doi.org/10.5516/NET.02.2013.519

Bertrand F., Bassi C., Bentivoglio F., Messie A., Tosello, A., Malo, J. Y., Preliminary Safety Analysis of the 2400 MW Gas-Cooled Fast Reactor, proceeding of ICAPP 2008, Anaheim, USA, June 8-12, 2008

Bertrand F., Bassi C., Bentivoglio F., Audubert F., Gueneau C., Rimpault G., Journeau C., Synthesis of safety studies carried out on the GFR2400, Nuclear Engineering and Design 253, pp 161-182, 2012

Bentivoglio F., Messié A., Geffraye G., Malo J.Y., Bertrand F., Plancq D., CATHARE simulation of transients for the 2400 MW gas fast reactor concept, proceeding of ICAPP 2009, Tokyo, Japan, May 10-14 2009

Bassi C., Azria P., Balmain M., Level 1 probabilistic safety assessment to support the design of the CEA 2400 MWth gas-cooled fast reactor. Nuclear Engineering and Design, Vol 240, Issue 11, pp. 3758-3780, 2010

Girardin G., Development of the control assembly pattern and dynamic analysis of the generation IV large gas-cooled fast reactor (GFR), Thèse de Doctorat de l'Ecole Polytechnique Fédérale de Lausanne (Suisse), soutenue le 9 juillet 2009

Bertrand F., Bensalah M., Gauthé P., Preliminary assessment with the CATHARE2 code of the transient behaviour of the ASTRID demonstrator depending on the design of its power conversion system, (NURETH-15), may 12-15 2013, Pise, Italy

Droin, J.B., Marie N., Bertrand F., Marrel A., Bachrata A., Design-oriented tool for Unprotected Loss Of Flow simulations in a Sodium Fast Reactor: Validation and application to stability analyses, Nuclear Engineering and Design, 361, May 2020, 110550
Marie N., Li S., Marrel A., Marquès M., Bajard S., Tosello A., Perez J., Grosjean B., Gerschenfeld A., Anderhuber M., Geffray C., Gorsse Y., Mauger G., Matteo L., VVUQ of a thermal-hydraulic multi-scale tool on unprotected loss of flow accident in SFR reactor, EPJ Nuclear Sci. Technol. 7, 3 (2021)
Bertrand F., Marie N., Prulhière G., Lecerf J., Seiler J.M., Comparison of the behaviour of two core designs for ASTRID in case of severe accidents, Nuclear Engineering and Design, Volume 297, February 2016, Pages 327-342
Bertrand F., Marie N., Bachrata A., Brun-Magaud V., Droin J.B., Manchon X., Herbreteau K., Farges B., Carluec B., Poumerouly S., Lemasson D., Status of severe accident studies at the end of the conceptual design of ASTRID: Feedback on mitigation features, Nuclear Engineering and Design, 326 (2018) 55–64
Kondo S., Yamano H., Tobita Y., Fujita S., Kamiyama K., Maschek W., Coste P., Pigny S., Louvet J., Phase 2 code assessment of SIMMER-III, JNC TN9400 2000-105, September 2000